2020 IEEE International Conference on Robotics and Automation (ICRA)
31 May - 31 August, 2020. Paris, France

A Connectivity-Prediction Algorithm and its Application in Active Cooperative Localization for Multi-Robot Systems

Liang Zhang[1], Zexu Zhang[1⋆], Roland Siegwart[2], Jen Jen Chung[2]

***Abstract*— This paper presents a method for predicting the probability of future connectivity between mobile robots with range-limited communication. In particular, we focus on its application to active motion planning for cooperative localization (CL). The probability of connection is modeled by the distribution of quadratic forms in random normal variables and is computed by the infinite power series expansion theorem. A finite-term approximation is made to realize the computational feasibility and three more modifications are designed to handle the adverse impacts introduced by the omission of the higher order series terms. On the basis of this algorithm, an active and CL problem with leader-follower architecture is then reformulated into a Markov Decision Process (MDP) with a one-step planning horizon, and the optimal motion strategy is generated by minimizing the expected cost of the MDP. Extensive simulations and comparisons are presented to show the effectiveness and efficiency of both the proposed prediction algorithm and the MDP model.**

I. INTRODUCTION

Active and cooperative localization is a promising paradigm for multi-robot systems (MRS) to work within GNSS denied environments, wherein the robots exploit an active, optimal motion strategy to obtain mutual observations that provide better spatial formation and more reliable information for a variety of practical applications in target tracking [1], environment monitoring [2], active perception and active SLAM [3], search and rescue [4] and so on.

An active motion policy aims at choosing optimal actions such that the system costs (rewards) can be minimized (maximized). However, in real-world deployments, robots usually suffer from uncertainty arising from both unknown external disturbances in motion and also noisy measurements from imperfect sensors. Precise prediction is much more critical and significant for MRS in cooperative localization (CL) scenarios since the robots are restricted to use only relative observations and communications to help localize themselves. Thus, the accuracy of their estimates highly depends on the efficiency and stability of communication and observation links, which are fragile and stochastic due to the presence of practical limitations and uncertainties.

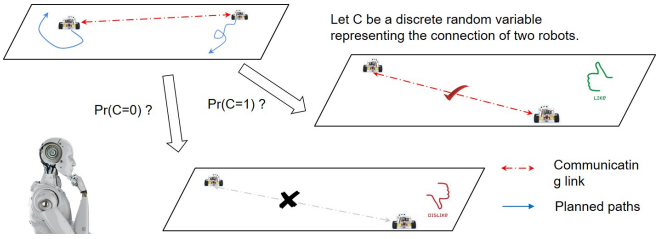

Fig. 1. Overall description of the problem. How to use known information at planning time to predict the future connection of two robots.

Early research on CL mainly focused on the theoretical realization [5]–[7] and experimental validation [8], [9] of the estimation and inference algorithms, in both centralized [6], [7] and distributed frameworks [10], [11]. Applications included optimal static formation [12], reallocation of communication resources among networks [13] and so on. More recently, CL in MRS have also been expanded for use in scenarios such as multi-robot target tracking [14]–[18], active information gathering [19]–[22] and autonomous exploration [23]–[26]. For some simple cases where the robots are assumed to have perfect knowledge about their positions, various algorithms have been proposed to derive optimal action polices. However, few methods are able to effectively handle robot uncertainty. One such example is the Belief Space Planning framework [27], [28] solved as a partial observable Markov decision process (POMDP) [23]–[29].

The prevailing methods for predicting the evolution of future team formations are mainly by 1): a deterministic connectivity computed by the prior estimated means, which has been shown to be unreliable and inconsistent, 2): a statistical connectivity whose distribution is computed by an approximated method e.g. an inversely proportional model to the mean distance between robots [23], [24], [29].

In this paper, an exact probability model of connectivity for a unit-disk communication model is developed and considered under the problem of CL using active motion planning under a leaders-followers architecture (CLAMP-LF). Under the assumption of Gaussian noise, we propose a novel algorithm to predict the probabilities of future connectivity for every pair of robots. This algorithm is developed under the basis of a series expansion formula of the quadratic positive form in a normal distribution, wherein an infinite summation of series is used to compute the cumulative distribution function (CDF). We propose several novel modifications to realize the balance of computational

Research supported in part by the National Natural Science Foundation of China under Granted 61374213 and 61573247 and the Open Foundation from Shanxi Key Laboratory of Integrated and Intelligent Navigation (SKLIIN-20180208). The authors gratefully acknowledge financial support from China Scholarship Council.

⋆Corresponding author: Zexu Zhang, zexuzhang@hit.edu.cn

[1] Liang Zhang and Zexu Zhang are with the Deep Space Exploration and Research Center, School of Astronautics, Harbin Institute of Technology, Harbin 150001, China. Liang Zhang is also a visiting student in Autonomous System Lab, ETH Zürich 8092, Switzerland when writing this paper. Zexu Zhang is also with the Shaanxi Key Laboratory of Integrated and Intelligent Navigation. liangzhangprc@gmail.com

[2] Jen Jen Chung and Roland Siegwart are with the Autonomous Systems Lab, ETH Zürich, Zürich 8092, Switzerland. {rsiegwart;chungj}@ethz.ch

tractability and the prediction accuracy. Our extensive simulation results show that the probability error remains within 7% given the underlying MRS environment. We compare our method to prior work that optimizes the actions of followers using the connectivity that is predicted only by the estimated means [30]. Results show that our proposed method can provide an average improvement of 53.9% on the leaders' pose uncertainties when the motion and observation models are both linear.

The contributions of this paper are twofold:

1) A novel predictive algorithm for the connectivity of robots given only the possible control actions and the current mean and covariance estimates.
2) The reformulation of the CLAMP-LF problem under the framework of an MDP with a one-step-ahead planning horizon.

II. Preliminaries and Problem statement

A. Preliminaries

CLAMP-LF: Consider a multi-robot system composed of N leaders, M followers and O anchors, where anchors know their global positions exactly whereas robots (both leaders and followers) can only obtain their initial positions and are required to jointly estimate their positions using only local, relative range measurements and the messages exchanged with their neighbors (other robots/anchors) via the interoceptive/exteroceptive sensors mounted on them. A robot (robots/anchors) can observe and communicate with others if their relative distance is smaller than a threshold ρ, which results in a time-varying connectivity within the MRS.

The motion model for the i-th robot and observation model for nodes i and j at time step k are denoted by,

$$\boldsymbol{p}_i(k+1) = f\left[\boldsymbol{p}_i(k), \boldsymbol{u}_i(k), \boldsymbol{w}_i\right], \tag{1}$$

$$\boldsymbol{z}_{i,j}(k) = h\left[\boldsymbol{p}_i(k), \boldsymbol{p}_j(k), \boldsymbol{v}_{i,j}\right] s_\rho\left[d_{i,j}(k)\right], \tag{2}$$

with zero-mean Gaussian process and measurement noise $\boldsymbol{w}_i \sim N(\boldsymbol{0}, \boldsymbol{Q})$ and $\boldsymbol{v}_{i,j} \sim N(\boldsymbol{0}, \boldsymbol{R})$, and known information matrices Q and R. $s_\rho(\cdot)$ is a binomial Regulation Function (RF) used to account for the loss or resurgence of the connection between robots i and j, which is given by,

$$s_\rho(d_{ij}(k)) = \begin{cases} 1, & d_{ij}(k) \le \rho \\ 0, & d_{ij}(k) > \rho, \end{cases} \tag{3}$$

and $d_{i,j}(k)$ is the true relative distance i.e.

$$d_{i,j}(k) = \left\| \boldsymbol{p}_i(k) - \boldsymbol{p}_j(k) \right\|_2. \tag{4}$$

For simplicity, the time index will be dropped when clear from the context. The dimensionality of measurement $\boldsymbol{z}_{i,j}$ is determined by the type of sensor.

Network Topology: Assume all robots and anchors are associated with the nodes of a time-varying undirected network topology graph $\mathcal{G}_k = \{\mathcal{V}, \mathcal{E}_k\}$ where $\mathcal{V}$ and $\mathcal{E}_k$ are the set of graph nodes and edges at time step k, respectively. The i-th node in the graph is denoted by $v_i, i \in \{1, \ldots, O+M+N\}$. The notation $(v_i, v_j) \in \mathcal{E}_k$ implies that $d_{i,j}(k) \le \rho$.

B. Problem Statement

At current time step k, the uncertainties of all robots are propagated by the Riccati recursion from the standard Extended Kalman Filter after obtaining the observation $\boldsymbol{z}_k := \{\boldsymbol{z}_{i,j}(k) | \forall i, j \in \mathcal{V}\}$,

$$\boldsymbol{P}_{k|k} = \left(\boldsymbol{P}_{k|k-1}^{-1} + \boldsymbol{H}_{\boldsymbol{z}_k}^T \boldsymbol{R}_k^{-1} \boldsymbol{H}_{\boldsymbol{z}_k}\right)^{-1}, \tag{5}$$

where the notation $H_{\boldsymbol{z}_k}$ is the Jacobian matrix of observations evaluated over the state of motion prediction $\hat{\boldsymbol{p}}_{k|k-1} := \{\hat{\boldsymbol{p}}_i(k|k-1) | \forall i \in \mathcal{V}\}$ where

$$\hat{\boldsymbol{p}}_i(k|k-1) = f[\hat{\boldsymbol{p}}_i(k-1|k-1), u(k-1)]$$

and the structure of $H_{\boldsymbol{z}_k}$ (i.e. existence of each row) is dependent on the network topology $\mathcal{G}_k$, which can be extracted from $\boldsymbol{z}_k$.

However, in order to choose an optimal action $\boldsymbol{u}_k^\star$ from the action space $\boldsymbol{A}_k$, it is common to virtually propagate the uncertainties by (5) over every possible action in $\boldsymbol{A}_k$ within the planning horizon (here we take one-time-step as an example) and then a cost (reward) function is defined according to the outcome of virtual propagation. The optimal control is selected to minimize (maximize) this cost (reward). Differing from the inference phase, we cannot determine $\boldsymbol{z}_{k+1}$ at time k. Thus the Jacobian matrix of observation $\boldsymbol{H}_{\boldsymbol{z}_{k+1}}$ cannot be fully determined during a planning session.

In the following, we focus on predicting the structure of $H_{\boldsymbol{z}_{k+1}}$, where an accurate and efficient algorithm to predict the probability of future topology is proposed. Before moving on, Provost and Mathai's theorem is presented, which is the basis of our algorithm:

Theorem 1: [31] Given the p-dimensional multivariate normal distribution $\boldsymbol{X} \sim N_p(\boldsymbol{\mu}, \boldsymbol{\Sigma})$, $\boldsymbol{\Sigma} > 0$ and its quadratic form $Y = Q(\boldsymbol{X}) = \boldsymbol{X}^T \boldsymbol{A} \boldsymbol{X}, \boldsymbol{A} = \boldsymbol{A}^T > 0$, let $\boldsymbol{b} = \boldsymbol{P}^T \boldsymbol{\Sigma}^{-\frac{1}{2}} \boldsymbol{\mu}$ and $\boldsymbol{\lambda} = [\lambda_1, ..., \lambda_p]^T$ be the eigenvalues of $\boldsymbol{\Sigma}^{\frac{1}{2}} A \boldsymbol{\Sigma}^{\frac{1}{2}}$, i.e. $P^T \boldsymbol{\Sigma}^{\frac{1}{2}} A \boldsymbol{\Sigma}^{\frac{1}{2}} P = diag(\boldsymbol{\lambda})$, $\boldsymbol{P}^T \boldsymbol{P} = \boldsymbol{I}$. Then the corresponding cumulative distribution function (CDF) of Y, that is $Pr\{Y \le y\}$, denoted by $F_p(\boldsymbol{\lambda}; \boldsymbol{b}; y)$, can be expanded as follows:

$$F_p(\boldsymbol{\lambda}; \boldsymbol{b}; y) = \sum_{k=0}^{\infty} (-1)^k c_k \frac{y^{\frac{p}{2}+k}}{\Gamma(\frac{p}{2}+k+1)}, \quad 0 < y < \infty, \tag{6}$$

where the coefficients c_k and d_k are defined by,

$$\begin{cases} c_0 = exp(-\frac{1}{2}\sum_{j=1}^{p} b_j^2) \prod_{j=1}^{p} (2\lambda_j)^{-\frac{1}{2}}, \\ c_k = \frac{1}{k} \sum_{r=0}^{k-1} d_{k-r} c_r, \quad k \ge 1, \end{cases} \tag{7}$$

$$d_k = \frac{1}{2} \sum_{j=1}^{p} (1 - k b_j^2)(2\lambda_j)^{-k}, \quad k \ge 1. \tag{8}$$

III. Connectivity prediction for two nodes

A. Modeling and finite-term approximation

Consider two robots whose true positions $\boldsymbol{p}_1, \boldsymbol{p}_2$ are distributed according to two normal distributions $\tilde{\boldsymbol{P}}_1 \sim N_2(\boldsymbol{\mu}_1, \boldsymbol{\Sigma}_1)$ and $\tilde{\boldsymbol{P}}_2 \sim N_2(\boldsymbol{\mu}_2, \boldsymbol{\Sigma}_2)$, respectively. The subtraction is also a normal distribution, i.e. $\Delta\tilde{\boldsymbol{P}} = \tilde{\boldsymbol{P}}_1 - \tilde{\boldsymbol{P}}_2 \sim N_\Delta(\boldsymbol{\mu}_1 -$

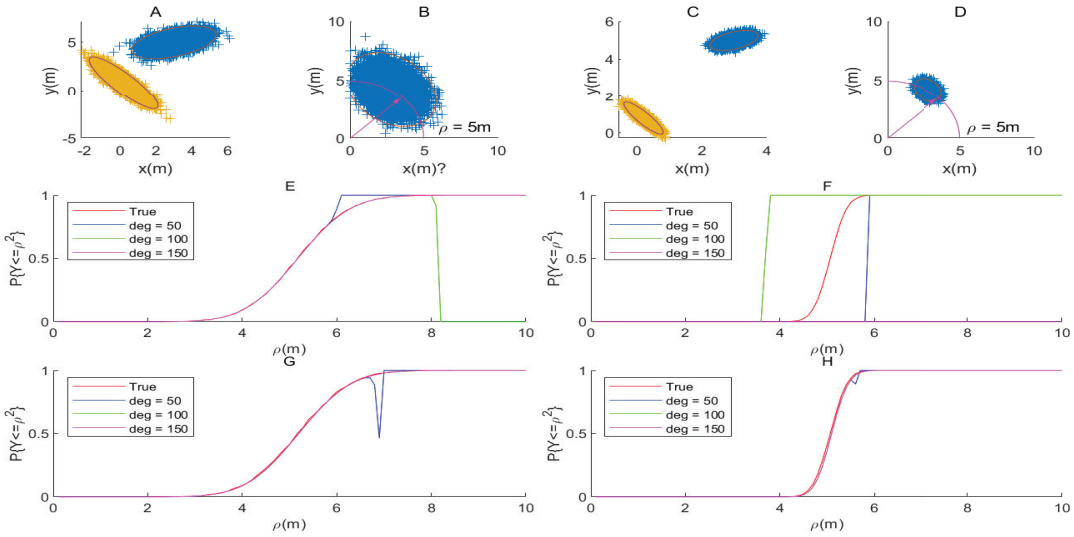

Fig. 2. Performance evaluation of the predictive algorithm for two nodes in two cases. {A,B}: Case 1, distribution of $\tilde{P}_1$ and $\tilde{P}_2$ in A, distribution of $\Delta\tilde{P}$ in B; {C,D}: Case 2 with ten times smaller covariance matrices for both tow nodes. {E,G}: Comparison of prediction performance before & after modifications for different deg under Case 1. {F,H}: Comparison of prediction performance before & after modifications for different deg under Case 2.

$\boldsymbol{\mu}_2, \boldsymbol{\Sigma}_1 + \boldsymbol{\Sigma}_2$). Thus, by denoting $\boldsymbol{X} = \Delta\tilde{\boldsymbol{P}} = [\Delta\tilde{\boldsymbol{P}}_x, \Delta\tilde{\boldsymbol{P}}_y]^T$, the square of the true distance computed by $d_{12} = \left\|\boldsymbol{p}_1 - \boldsymbol{p}_2\right\|_2$ can be equally represented by a quadratic random variable $Y = Q(\boldsymbol{X}) = \Delta\tilde{\boldsymbol{P}}_x^2 + \Delta\tilde{\boldsymbol{P}}_y^2 = \boldsymbol{X}^T\boldsymbol{A}\boldsymbol{X}$, where $\boldsymbol{A} = \boldsymbol{I}$.

Let a discrete random variable C be the state of connectivity between these two robots, where $C = 1$ if they can observe and communicate with each other and $C = 0$ if they can't. Given the maximum communication range ρ, then the relationship between the random variables Y and C is,

$$Pr\,(C = 1) = Pr\left(Y \le \rho^2\right). \tag{9}$$

As a result, it is straightforward to use Theorem 1 with dimensionality $p = 2$ to predict the probability of connection between two nodes, given only the estimates of means and covariance matrices of both positions. However, Theorem 1 needs to compute an infinite summation of power series terms, which is intractable for practical applications. One instinctive approach is to sum only a finite but sufficient number of terms. This means replacing (6) with

$$F_p(\boldsymbol{\lambda}; \boldsymbol{b}; y) = \sum_{k=0}^{deg} (-1)^k c_k \frac{y^{\frac{p}{2}+k}}{\Gamma(\frac{p}{2}+k+1)}, \quad 0 < y < \infty, \tag{10}$$

where deg is a proper maximum degree for our algorithm to be determined. However, this method will introduce errors to the calculation of F_p compared with the original infinite sum version in Theorem 1. Thus, the main difficulty that remains is how to maintain the balance between the tractability and predictive accuracy of our algorithm.

B. Drawbacks and solutions

In this subsection, we focus on reducing the predictive error of F_p based on the finite-terms equation in (10). We observed two main drawbacks caused by the omission of the higher order terms from the simulation in Figs. 2E–H.

The first problem is that the forecast of $Pr\left(Y \le \rho^2\right)$ computed from (10) will dramatically tend to ∞ or $-\infty$ when the independent variable ρ is greater than a certain threshold defined by an **inflection point** (InP). The tendency to positive/negative is determined by the deg chosen and used in (10). This phenomenon is shown in Fig. 2E. From the figure, we can see that our method can only estimate the probability correctly and stably within the stable set [0 InP].

The reason behind this problem is clear from the equation (10), where the term $(-1)^k$ drives the two consecutive polynomials, whose powers are k and k+1, in totally opposed directions and thus the overall sum of infinite terms in (6) can be bounded in [0 1]. Since those terms after deg have been eliminated in (10), the approximated value of F_p can no longer be stable after $\rho >$ InP.

The second disadvantage is shown in Fig. 2H when the covariance matrix of $\Delta\tilde{P}$ is very small or is near singularity. At this point, (10) cannot estimate the probability on the **increasing surface** (here, when $4 < \rho < 6$) regardless the value of deg. To explain this degeneration, we know that the computation of coefficients c_k and d_k requires the reciprocal eigenvalues (c_0 in (7)) and the inverse of the covariance matrices ($\boldsymbol{b} = P^T\Sigma^{-\frac{1}{2}}\boldsymbol{\mu}$), which makes those coefficients abnormally large if the covariance matrix is not well constructed, causing the prediction to diverge from [0 1] much easier and faster. However, it is still important to get the accurate probability of connection when the mean distance lies around the communicating range.

Based on our finite-term approximation (10), three solutions are proposed for those problems:

Concerning the first drawback, two corrections are developed here. On the one hand, **3δ regulation** is applied by simply assigning the probability to 1 if the ranging maximum ρ is larger than the 3δ area, and 0 if less, regardless of the output from (10). This originates from the fact that $\Delta\tilde{P}$ is a two-dimensional normal distribution, thus, 99.7% of the sampled points lie in the 3δ confidence area. On the other hand, if the output of F_p is negative but larger than the mean distance when ρ is within [ρ_1 ρ_2], which indicates F_p is beyond the stable set, then the probability will be assigned

to 1. This procedure is named **saltation regulation**.

Regarding the second problem, the covariance is expanded by multiplying a proper coefficient to protect our coefficients from being abnormally large,which is referred to as **Approximate Covariance Expansion** (ACE) in the rest of this paper.

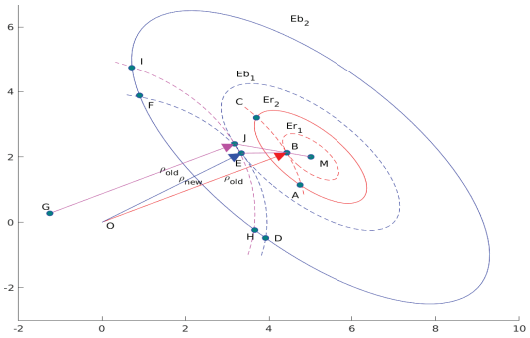

Fig. 3. Covariance Expansion for addressing the second drawback

A detailed description of ACE is shown in Fig. 3 where the red solid ellipse Er_2 represents the 3δ confidence area corresponding to the covariance matrix $\Sigma = \Sigma_1 + \Sigma_2$ of $\Delta\bar{P}$. Under such circumstances, Σ is multiplied by a coefficient $co \geq 1$ and therefore is enlarged into the blue solid ellipse Eb_2. Taking the maximum communication distance to be ρ_{old} where its ranging circle from the origin O with radius ρ_{old} intercepts with the 3δ area of Er_2, there exists a smaller ellipse Er_1 that is tangent to this ranging circle. After enlargement, this tangent ellipse Er_1 is extended to Eb_1 with the same proportion co. Hence, initially, the probability of connection between those two robots is,

$$F_p(\boldsymbol{\lambda}; \boldsymbol{b}; \rho_{old}) \approx \frac{S(\widehat{ABC} \cap \mathrm{Er}_2)}{S(\mathrm{Er}_2)}, \tag{11}$$

where $S(\cdot)$ stands for the shape's area. $F_p(\boldsymbol{\lambda}; \boldsymbol{b}; \rho_{old})$ is generated by equation (10). After expansion, we get

$$\frac{S(\widehat{ABC} \cap \mathrm{Er}_2)}{S(\mathrm{Er}_2)} = \frac{S(\widehat{HJI} \cap \mathrm{Eb}_2)}{S(\mathrm{Eb}_2)}. \tag{12}$$

Thus, by taking the approximation

$$\frac{S(\widehat{DEF} \cap \mathrm{Eb}_2)}{S(\mathrm{Eb}_2)} \approx \frac{S(\widehat{HJI} \cap \mathrm{Eb}_2)}{S(\mathrm{Eb}_2)}, \tag{13}$$

we can use another CDF, $F_p(co\boldsymbol{\lambda}; \frac{1}{\sqrt{co}}\boldsymbol{b}; \rho_{new})$, with a new ranging circle ρ_{new} to approximate the original probability $F_p(\boldsymbol{\lambda}; \boldsymbol{b}; \rho_{old})$, where we have the relationship,

$$F_p(co\boldsymbol{\lambda}; \frac{1}{\sqrt{co}}\boldsymbol{b}; \rho_{new}) \approx \frac{S(\widehat{DEF} \cap \mathrm{Eb}_2)}{S(\mathrm{Eb}_2)}. \tag{14}$$

Therefore, the probability can be computed by a larger covariance matrix,

$$F_p(co\boldsymbol{\lambda}; \frac{1}{\sqrt{co}}\boldsymbol{b}; \rho_{new}) \approx F_p(\boldsymbol{\lambda}; \boldsymbol{b}; \rho_{old}). \tag{15}$$

From the basic geometric similarity shown in Fig. 3, the alternative circling radius ρ_{new} can be calculated under the assumption that points J and E are approximately equal, which results in,

$$\rho_{new} = \left\| (1 - \sqrt{co})\overrightarrow{OM} + \sqrt{co}\overrightarrow{OB} \right\|_2, \tag{16}$$

where $\overrightarrow{OM}$, $\overrightarrow{OB}$ are the vectors combining the corresponding points shown in Fig. 3. Moreover, we have $\left\|\overrightarrow{OM}\right\|_2 = d_m$ which is the mean distance and $\left\|\overrightarrow{OB}\right\|_2 = \rho_{old}$. However, it is usually still difficult to compute the tangent point B and hence we can further assume that points O, B, M are collinear, so that we can use a simpler formula to compute ρ_{new} as,

$$\rho_{new} \approx (1 - \sqrt{co})d_m + \sqrt{co}\rho_{old}. \tag{17}$$

It should be noted that there are various ways to choose a proper co. In the following algorithm, we calculate co by expanding the covariance matrix to a new one whose smallest eigenvalue is larger than 1.

C. Algorithm

Algorithm 1: Probability of Connection

Result: $Pr(Y < \rho_{old}^2)$
Data: $\boldsymbol{\mu}_1, \boldsymbol{\mu}_2, \boldsymbol{\Sigma}_1, \boldsymbol{\Sigma}_2, \boldsymbol{u}_1, \boldsymbol{u}_2, \boldsymbol{R}_1, \boldsymbol{R}_2, \rho_{old}, deg$;
$\boldsymbol{\mu}_1(k+1|k) = \boldsymbol{\mu}_1 + \boldsymbol{u}_1$, $\boldsymbol{\mu}_2(k+1|k) = \boldsymbol{\mu}_2 + \boldsymbol{u}_2$;
$\boldsymbol{\Sigma}_1(k+1|k) \leftarrow$ Motion update $(\boldsymbol{\Sigma}_1, R_1)$;
$\boldsymbol{\Sigma}_2(k+1|k) \leftarrow$ Motion update $(\boldsymbol{\Sigma}_2, R_2)$;
$\boldsymbol{\mu} = \boldsymbol{\mu}_1(k+1|k) - \boldsymbol{\mu}_2(k+1|k)$;
$\boldsymbol{\Sigma} = \boldsymbol{\Sigma}_1(k+1|k) + \boldsymbol{\Sigma}_2(k+1|k)$;
$[\rho_{3\delta}^{min} \rho_{3\delta}^{max}] \leftarrow 3\delta$ area identification ;
if $\rho_{old} < \rho_{3\delta}^{min}$ **then**
  Return $Pr(Y < \rho_{old}^2) = 0$;
end
if $\rho_{old} > \rho_{3\delta}^{max}$ **then**
  Return $Pr(Y < \rho_{old}^2) = 1$;
end
$co = \dfrac{1}{min(eig(\boldsymbol{\Sigma}))}$;
if $co < 1$ **then**
  $co = 1, \rho_{new} = \rho_{old}$;
else
  $\rho_{new} \leftarrow (17)$;
end
$\boldsymbol{\Sigma} = co \times \boldsymbol{\Sigma}$;
$\boldsymbol{b} = \boldsymbol{P}^T \boldsymbol{\Sigma}^{-\frac{1}{2}} \boldsymbol{\mu}; \boldsymbol{\lambda} = diagonal(\boldsymbol{P}^T \boldsymbol{\Sigma} \boldsymbol{P})$, $\boldsymbol{P}^T \boldsymbol{P} = \boldsymbol{I}$;
while $r \leq deg$ **do**
  $c_r \leftarrow (7), r = 0, ..., deg$;
  $d_r \leftarrow (8), r = 1, ..., deg$;
  $y_r = (-1)^r \dfrac{\rho_{new}^{r+1}}{\Gamma(r+2)}, r = 0, ..., deg$;
end
$F_p(\boldsymbol{\lambda}; \boldsymbol{b}; \rho_{new}) \leftarrow (10)$;
$Pr(Y < \rho_{old}^2) = F_p(\boldsymbol{\lambda}; \boldsymbol{b}; \rho_{new})$;
if $Pr(Y < \rho_{old}^2) < 0$ & $\rho_{old} > d_{mean}$ **then**
  $Pr(Y < \rho_{old}^2) = 1$;
end
Return $Pr(Y < \rho_{old}^2)$

The probability prediction algorithm for the future connectivity between two nodes is summarized in Algorithm 1 and takes as input the current estimates of mean positions

$(\boldsymbol{\mu}_1, \boldsymbol{\mu}_2)$, covariance matrices (Σ_1, Σ_2), the possible control action $(\boldsymbol{u}_1, \boldsymbol{u}_2)$ as well as the covariance of motion noise (R_1, R_2). The sequence of this algorithm is as follows: lines 6–12 describe the realization of 3δ regulation; ACE is presented within lines 13–26; saltation regulation corresponds to lines 28–30.

IV. Application to CLAMP-LF

In this section, Algorithm 1 is applied to the CLAMP-LF problem, which is formally reformulated into a one-step finite state MDP.

A: For the proposed MRS, we have $N_n = O+M+N$ nodes, and thus have $N_{GC} = \frac{N_n(N_n-1)}{2}$ possible connections. Let's denote the i-th connection by C_i where $i \leq N_{GC}$.

B: The MDP state is the combination of all possible pairwise connection statuses in the graph $\mathcal{G}_k$, which has the notation $S = [C_1, C_2, ..., C_{N_{GC}}]^T$. Since each connection is either 1 or 0, the MDP has in total $N_s = 2^{N_{GC}}$ states. The state space is given by $\mathbf{S} = \{S_1, S_2, ..., S_{N_s}\}$.

C: The random variable $\mathbf{X}_k \in \mathbf{S}$ represents the state of the MRS graph $\mathcal{G}_k$ at time step k. The overall control space is $\mathbf{A}_k = \mathbf{A}_k^1 \times ... \times \mathbf{A}_k^N$.

D: Given a control action $a \in \mathbf{A_k}$, the transition model is a $N_s \times N_s$ probability matrix denoted as $\mathbf{P}_a(S_i, S_j) = P(\mathbf{X}_{k+1} = S_j | \mathbf{X}_k = S_i, u = a), \forall S_j, S_i \in \mathbf{S}$. It is updated according to,

$$\mathbf{P}_a(S_i, S_j) = \prod_{r=1}^{N_s} Pr\{C_r = S_j(r)\}, \tag{18}$$

where each element in the product on right hand side is repeatedly computed by Algorithm 1.

E: Each transition emits a cost $\mathbf{R}_a(S_i, S_j)$, which is the predicted covariance uncertainties of all leaders,

$$\begin{aligned} &\mathbf{R}_a(S_i, S_j) = trace(\hat{\boldsymbol{P}}_{k+1|k+1})_{L_k} \\ &\hat{\boldsymbol{P}}_{k+1|k+1} = \left(\boldsymbol{P}_{k+1|k}^{-1} + \boldsymbol{H}_{k+1|k}^T(S_j)\boldsymbol{Q}_k^{-1}\boldsymbol{H}_{k+1|k}(S_j)\right)^{-1}. \end{aligned} \tag{19}$$

With the definition processes A-E, we get the MDP denoted by a 4-tuple $\langle \mathbf{S}, \mathbf{A}, \mathbf{P}, \mathbf{R} \rangle$. The optimal policy $\pi^\star$ for all followers is defined by minimizing the expected one-step-ahead cost, which is formulated as,

$$\pi^\star(S) = \text{argmin}_a \left\{ \sum_{j=1}^{N_s} \mathbf{P}_a(S, S_j)\mathbf{R}_a(S, S_j) \right\}. \tag{20}$$

It is worthwhile to note that the current state cannot completely account for the cost function in (19). It is also affected by the informative matrix of motion noise, $\boldsymbol{R}_k$, and the measurement Jacobian, $\boldsymbol{H}_{k+1|k}$. Thus, if the motion model and observation model in (1)-(2) are linear, this definition A-E holds strictly. However, if the models are nonlinear, in the algorithm, they are all linearized by the first-order Taylor series expansion approximation over the estimated states, which introduces estimated stochastic values to the Jacobian matrices of both observation and motion and thus results in the correlation between the cost and the random values.

V. Simulation Results and Discussion

A. Performance of the algorithm

The performance of Algorithm 1 when a predicting single connection is compared with the original finite-term approximation (10). The results are shown in Fig. 2. It can be seen from the comparisons of Fig. 2{E, G} and {F, H}, that our proposed algorithm improves the performance of the probability prediction procedure.

Next, we test the performance of simultaneously predicting multiple connections using our algorithm when applied to MRS. In the following simulation, three robots (r_1, r_2, r_3) and one anchor (A) are used, thus we have in total 6 possible observation links. The relative distances are initialized in Table I. The covariance matrices $\boldsymbol{R}_i, i = 1,2,3$ are all set to be $diag([0.04, 0.04])$. The maximum ranging distance of our communication and measurement devices is set to $\rho = 5$m.

TABLE I
Initial distance and link configurations

Index	1	2	3	4	5	6
Nodes	$\{A,r_1\}$	$\{A,r_2\}$	$\{A,r_3\}$	$\{r_1,r_2\}$	$\{r_1,r_3\}$	$\{r_2,r_3\}$
Dis(m)	3	5.83	4.47	3.61	4.12	3.16

Given this setup, each robot first generates a control action, the distance to travel for each control is limited to under 1m regardless of the direction. Each robot predicts its next position by the motion update, and then uses its predicted values to calculate the probabilities of connections according to Algorithm 1. Meanwhile this control command is corrupted by a sampled noise from $\boldsymbol{R}_i$ to get the true positions. This corruption process is repeated 1000 times to count the frequencies of true link status, which are used as **ground-truth** of the connection probabilities under this control and are compared to the outputs of the proposed algorithm. In total, we generated 200 control actions. The distribution of errors between real frequencies and our predicted probabilities from Algorithm 1 is shown in Fig. 4

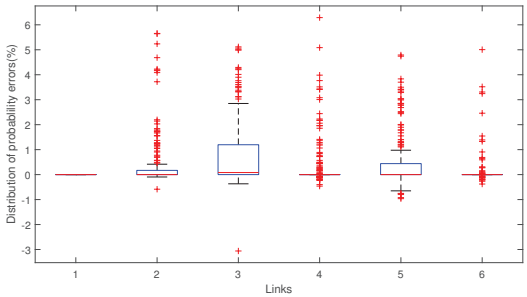

Fig. 4. Distribution of probability errors

In Fig. 4, the upper bound of the probability error for future connections is no more than 7%, validating the approximations made in the former section.

B. CLAMP-LF Simulation

In this section, the optimal policy in (20) is applied to the CLAMP problem and is compared against the optimal method in our previous work [30], which only uses an A-optimality indicator computed by the estimated means. Both

linear and nonlinear measurement models are used and the robots are modeled as points with motion given by,

$$\boldsymbol{p}_i(k+1) = \boldsymbol{p}_i(k) + \boldsymbol{u_i}(k) + \boldsymbol{w}_i. \tag{21}$$

A linear measurement model assumes the robot can directly measure relative distance along both x and y directions to any other robot, i.e.

$$\boldsymbol{z}_{i,j}(k) = \boldsymbol{p}_i(k) - \boldsymbol{p}_j(k) + \boldsymbol{v}_{i,j}. \tag{22}$$

Here the dimensionality of the known covariance matrix $R_{i,j}$ is 2×2. The nonlinear measurement model that we test can only measure the distance along the communication direction,

$$z_{i,j} = ||\boldsymbol{p}_i(k) - \boldsymbol{p}_j(k)||_2 + v_{i,j}, \tag{23}$$

where the measurement and noise are scalar. Taking the overall concatenated position state as $\boldsymbol{p} = [\boldsymbol{p}_1, \boldsymbol{p}_2, ..., \boldsymbol{p}_{N+M}]^T$, the basic row-block for the r-th link in the observation Jacobian connecting nodes i and j for the linear model is,

$$\boldsymbol{H}_o(r,:) = \left[0_{2\times2}, ..., \boldsymbol{I}^i_{2\times2}, 0_{2\times2}, ..., -\boldsymbol{I}^j_{2\times2}, 0_{2\times2}, ..., 0_{2\times2}\right], \tag{24}$$

where $I^i_{2\times2}$ lies on the i-th column and $I^j_{2\times2}$ on the j-th column. Whereas, for the nonlinear measurement model, the basic row-block is,

$$\boldsymbol{H}_o(r,:) = \left[\boldsymbol{0}_{1\times2}, ..., \boldsymbol{h}^i_0, \boldsymbol{0}_{1\times2}, ..., \boldsymbol{h}^j_0, \boldsymbol{0}_{1\times2}, ..., \boldsymbol{0}_{1\times2}\right], \tag{25}$$

where $\boldsymbol{h}^j_0 = -\boldsymbol{h}^i_0 = [\frac{p^x_i - p^x_j}{d_{i,j}}, \frac{p^y_i - p^y_j}{d_{i,j}}]$ and p^x_i, p^y_i are the elements in the position vector of robot i. Since we can only get the estimated values of positions at planning time, $\boldsymbol{h}^i_o$ and $\boldsymbol{h}^j_o$ are essentially stochastic.

The setup of the MRS and the initial configurations are the same as in Table I. As in our prior work [30], the leader's high level task is to reach a goal position in the opposite diagonal corner of the environment, and it moves directly towards the goal. The action space for the i-th robot is defined as $\mathbf{A}_i = \{\text{North, South, East, West, DoNothing}\}$. Each movement in the space is limited to 1m. The degree of (10) in our algorithm is set to 150.

Simulation results are shown in Fig. 5 and Fig. 6 where our proposed method is denoted by 'OS-MDP' and the optimization method in our previous work [30] is referred as 'A-optimality'. Both linear and nonlinear measurement models are simulated for 200 trials. Table II shows the processed statistical results in the final step.

TABLE II

DISTRIBUTION OF THE FINAL STEP OVER 200 TRIALS

	Linear Model		Nonlinear Model	
	Mean	Variance	Mean	Variance
OS-MDP	**0.0827**	**0.0026**	**0.3218**	**0.53×10^{-3}**
A-optimality	0.1794	0.0163	0.3415	2.73 ×10^{-3}
Improvement	53.9%	82.3%	5.8%	80.4%

As shown in these figures, using our proposed method, the leader's uncertainty is lower and has a lighter tail. Therefore, the optimal policy from (20) can improve the localization performance for both types of observation model.

Specifically, for linear models, our proposed method surpasses the best performance of the A-optimality method in

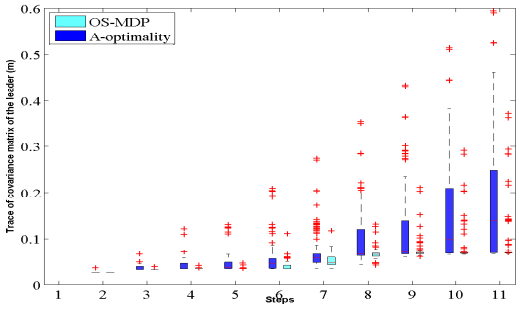

Fig. 5. Evolution of the leader's localization uncertainty for a **Linear Observation model** (22)

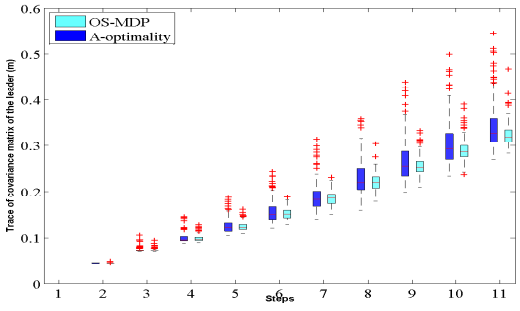

Fig. 6. Evolution of the leader's localization uncertainty for a **Nonlinear Observation model** (23)

over 75% of the trials at the final step. The upper bound of outliers is also sparser and lower than that of the A-optimality method. For nonlinear models, however, the improvement is a little smaller with respect to the means of all trials in the final step. The reason, as mentioned in the previous section and summarized again here, is that the linearized Jacobians of both motion and observation will introduce stochasticity into the MDP model. The consequence of which is that the MDP cost does not completely depend on the state. However, our proposed policy can substantially improve the variance of the uncertainty, which helps reduce the long tails from which the A-optimality method suffers. Despite the aforementioned advantages in the nonlinear case, we notice that the proposed method also suffers from a worse "best solution" than the A-optimality approach. This is partly due to the errors of the predictive algorithm introduced by the approximations made to ensure tractability. This is left as an open problem for further investigation in the future.

VI. CONCLUSIONS

In this paper, we proposed a novel algorithm to predict the probability of future connections across a MRS based on only the current estimates of positions. Our contributions in this part mainly focus on the improvement of the predictive accuracy as well as tractability through a finite-terms approximation. Using the proposed prediction algorithm, the CLAMP-LF problem was then cast as a one-step MDP problem and the optimal policy for all followers was designed in order to minimize the expected localization uncertainty of the leaders. Future work will concentrate on further improvements in nonlinear cases, distributing the motion strategy and applications to large scale MRS.

REFERENCES

[1] A. Khan, B. Rinner, and A. Cavallaro, "Cooperative robots to observe moving targets," *IEEE transactions on cybernetics*, vol. 48, no. 1, pp. 187–198, 2016.

[2] V. Kumar, D. Rus, and S. Singh, "Robot and sensor networks for first responders," *IEEE Pervasive computing*, vol. 3, no. 4, pp. 24–33, 2004.

[3] C. Cadena, L. Carlone, H. Carrillo, Y. Latif, D. Scaramuzza, J. Neira, I. Reid, and J. J. Leonard, "Past, present, and future of simultaneous localization and mapping: Toward the robust-perception age," *IEEE Transactions on robotics*, vol. 32, no. 6, pp. 1309–1332, 2016.

[4] N. Patwari, J. N. Ash, S. Kyperountas, A. O. Hero, R. L. Moses, and N. S. Correal, "Locating the nodes: cooperative localization in wireless sensor networks," *IEEE Signal processing magazine*, vol. 22, no. 4, pp. 54–69, 2005.

[5] S. I. Roumeliotis and G. A. Bekey, "Distributed multirobot localization," *IEEE transactions on robotics and automation*, vol. 18, no. 5, pp. 781–795, 2002.

[6] S. I. Roumeliotis and I. M. Rekleitis, "Analysis of multirobot localization uncertainty propagation," in *Proceedings 2003 IEEE/RSJ International Conference on Intelligent Robots and Systems (IROS 2003)(Cat. No. 03CH37453)*, vol. 2. IEEE, 2003, pp. 1763–1770.

[7] A. I. Mourikis and S. I. Roumeliotis, "Performance analysis of multirobot cooperative localization," *IEEE Transactions on robotics*, vol. 22, no. 4, pp. 666–681, 2006.

[8] R. Kurazume and S. Hirose, "An experimental study of a cooperative positioning system," *Autonomous Robots*, vol. 8, no. 1, pp. 43–52, 2000.

[9] N. Trawny and T. Barfoot, "Optimized motion strategies for cooperative localization of mobile robots," in *IEEE International Conference on Robotics and Automation, 2004. Proceedings. ICRA'04. 2004*, vol. 1. IEEE, 2004, pp. 1027–1032.

[10] R. Olfati-Saber, "Distributed kalman filtering for sensor networks," in *2007 46th IEEE Conference on Decision and Control*. IEEE, 2007, pp. 5492–5498.

[11] P. Yang, R. A. Freeman, and K. M. Lynch, "Distributed cooperative active sensing using consensus filters," in *Proceedings 2007 IEEE International Conference on Robotics and Automation*. IEEE, 2007, pp. 405–410.

[12] Y. S. Hidaka, A. I. Mourikis, and S. I. Roumeliotis, "Optimal formations for cooperative localization of mobile robots," in *Proceedings of the 2005 IEEE International Conference on Robotics and Automation*. IEEE, 2005, pp. 4126–4131.

[13] A. I. Mourikis and S. I. Roumeliotis, "Optimal sensor scheduling for resource-constrained localization of mobile robot formations," *IEEE Transactions on Robotics*, vol. 22, no. 5, pp. 917–931, 2006.

[14] K. Zhou and S. I. Roumeliotis, "Optimal motion strategies for range-only constrained multisensor target tracking," *IEEE Transactions on Robotics*, vol. 24, no. 5, pp. 1168–1185, 2008.

[15] E. Stump, V. Kumar, B. Grocholsky, and P. M. Shiroma, "Control for localization of targets using range-only sensors," *The International Journal of Robotics Research*, vol. 28, no. 6, pp. 743–757, 2009.

[16] G. H. Jajamovich and X. Wang, "Joint multitarget tracking and sensor localization in collaborative sensor networks," *IEEE Transactions on Aerospace and Electronic Systems*, vol. 47, no. 4, pp. 2361–2375, 2011.

[17] K. Zhou and S. I. Roumeliotis, "Multirobot active target tracking with combinations of relative observations," *IEEE Transactions on Robotics*, vol. 27, no. 4, pp. 678–695, 2011.

[18] F. Morbidi and G. L. Mariottini, "Active target tracking and cooperative localization for teams of aerial vehicles," *IEEE transactions on control systems technology*, vol. 21, no. 5, pp. 1694–1707, 2012.

[19] J. Le Ny and G. J. Pappas, "On trajectory optimization for active sensing in gaussian process models," in *Proceedings of the 48h IEEE Conference on Decision and Control (CDC) held jointly with 2009 28th Chinese Control Conference*. IEEE, 2009, pp. 6286–6292.

[20] N. Atanasov, J. Le Ny, K. Daniilidis, and G. J. Pappas, "Information acquisition with sensing robots: Algorithms and error bounds," in *2014 IEEE International Conference on Robotics and Automation (ICRA)*. IEEE, 2014, pp. 6447–6454.

[21] X. Lan and M. Schwager, "Rapidly exploring random cycles: Persistent estimation of spatiotemporal fields with multiple sensing robots," *IEEE Transactions on Robotics*, vol. 32, no. 5, pp. 1230–1244, 2016.

[22] B. Schlotfeldt, D. Thakur, N. Atanasov, V. Kumar, and G. J. Pappas, "Anytime planning for decentralized multirobot active information gathering," *IEEE Robotics and Automation Letters*, vol. 3, no. 2, pp. 1025–1032, 2018.

[23] V. Indelman, "Towards multi-robot active collaborative state estimation via belief space planning," in *2015 IEEE/RSJ International Conference on Intelligent Robots and Systems (IROS)*. IEEE, 2015, pp. 4620–4626.

[24] V. Indelman, L. Carlone, and F. Dellaert, "Planning in the continuous domain: A generalized belief space approach for autonomous navigation in unknown environments," *The International Journal of Robotics Research*, vol. 34, no. 7, pp. 849–882, 2015.

[25] T. Regev and V. Indelman, "Multi-robot decentralized belief space planning in unknown environments via efficient re-evaluation of impacted paths," in *2016 IEEE/RSJ International Conference on Intelligent Robots and Systems (IROS)*. IEEE, 2016, pp. 5591–5598.

[26] ——, "Decentralized multi-robot belief space planning in unknown environments via identification and efficient re-evaluation of impacted paths," *Autonomous Robots*, vol. 42, no. 4, pp. 691–713, 2018.

[27] C. H. Papadimitriou and J. N. Tsitsiklis, "The complexity of markov decision processes," *Mathematics of operations research*, vol. 12, no. 3, pp. 441–450, 1987.

[28] J. Van Den Berg, S. Patil, and R. Alterovitz, "Motion planning under uncertainty using iterative local optimization in belief space," *The International Journal of Robotics Research*, vol. 31, no. 11, pp. 1263–1278, 2012.

[29] V. Indelman, "Cooperative multi-robot belief space planning for autonomous navigation in unknown environments," *Autonomous Robots*, vol. 42, no. 2, pp. 353–373, 2018.

[30] L. Zhang, Z. Zhang, R. Siegwart, and J. J. Chung, "Optimized motion strategy for active target localization of mobile robots with time-varying connectivity," in *2019 International Symposium on Multi-Robot and Multi-Agent Systems (MRS)*. IEEE, 2019, pp. 185–187.

[31] S. B. Provost and A. Mathai, *Quadratic forms in random variables: theory and applications*. M. Dekker, 1992.